Hydrous Manganese Dioxide Nanowall Arrays Growth and Their Li^+ Ions Intercalation Electrochemical Properties

Dawei Liu,[†] Qifeng Zhang,[†] Peng Xiao,[†,⊥] Betzaida B. Garcia,[†] Qing Guo,[‡] Richard Champion,[§] and Guozhong Cao*[,†]

Department of Materials Science and Engineering, Department of Mechanical Engineering, and Department of Chemical Engineering, University of Washington, Seattle, Washington 98195, and Department of Physics, Chongqing University, P. R. China

Received July 26, 2007. Revised Manuscript Received November 13, 2007

Nanowall arrays of hydrous manganese dioxide $MnO_2 \cdot 0.5H_2O$ were deposited on cathodic substrates by the potentiostatic method from a mixed aqueous solution of manganese acetate and sodium sulfate, and the Li^+ ions intercalation properties of such nanowall arrays were studied. The deposition was induced by a change of local pH resulting from electrolysis of H_2O. Composition of this new nanowall structure was investigated by means of combined XRD, XPS, and TGA and determined to be hydrous manganese dioxide. SEM study revealed that the $MnO_2 \cdot 0.5H_2O$ nanowall arrays were homogeneous across the entire substrate of top thicknesses that varied from 50 to 100 nm with identical depth. The nanowall arrays of hydrous manganese dioxide exhibited an initial capacity of 270 mAh/g with a reversible capacity maintained at 220 mAh/g at the 50th charge/discharge cycle in the Li^+ ions intercalation capacity measurement at a high charge/discharge rate of 0.1 mA/cm^2 (C/2, 76 mAh/g). This greatly enhanced Li^+ ions intercalation capacity is ascribed to the large active surface area of the nanowall arrays and a short facile diffusion path for Li^+ ions. The nanowall arrays of hydrous manganese dioxide also displayed an improved cyclic stability attributed to the reduced strain accumulated in these nanostructures during Li^+ ions intercalation.

1. Introduction

Manganese dioxide has long been a favorable candidate for the applications in electronic devices, such as supercapacitors[1] and Zn/MnO_2 batteries,[2] due to its low cost and limited environmental impact.[3] Because of these advantages, manganese dioxide is considered to be one of the best cathode materials for Li^+ ions batteries. However, compared to other transition metal oxides, such as vanadium pentoxide whose films can deliver a discharge capacity of up to 300 mAh/g,[4] the films of manganese dioxide deliver a typically lower discharge capacity of <120 mAh/g.[5] This shortfall in capacity limits its potential application in Li^+ ions batteries. Several methods to improve the Li^+ ions capacity have been explored.[6,7] One major effort has been to increase the active surface area of manganese dioxide and, thus, allow for a short facile solid-state diffusion path for Li^+ ions.[8] Appropriately fabricated nanostructures would satisfy such requirements and thus offer much enhanced Li^+ ions intercalation capability and improved charge/discharge kinetics. Wang et al. have shown that nanorod, nanotube, and nanocable arrays of vanadium pentoxide exhibited a significantly higher discharge capacity than V_2O_5 films.[9,10] Nanorods or nanowires of manganese dioxide have also been fabricated by template-based sol–gel[11] and electrochemical deposition[12,13] methods with enhanced Li^+ ions intercalation properties compared with bulk films. In addition, since hydrous manganese dioxide has been studied for capacitor applications,[14] amorphous films of hydrous manganese dioxide were also investigated in Li^+ ions battery applications[15] to improve the charge/discharge cyclic stability. Template-based nanowires of hydrous manganese dioxide

* To whom correspondence should be addressed. E-mail: gzcao@u.washington.edu.
[†] Department of Materials Science and Engineering, University of Washington.
[‡] Department of Mechanical Engineering, University of Washington.
[§] Department of Chemical Engineering, University of Washington.
[⊥] Chongqing University.

(1) Reddy, R. N.; Reddy, R. G. *J. Power Sources* **2004**, *132*, 315.
(2) Minakshi, M.; Singh, P.; Issa, T. B.; Thurgate, S.; Marco, R. D. *J. Power Sources* **2006**, *153*, 165.
(3) Johnson, C. S. *J. Power Sources* **2007**, *165*, 559.
(4) Wang, Y.; Cao, G. Z. *Electrochim. Acta* **2006**, *51*, 4865.
(5) Johnson, C. S.; Dees, D. W.; Mansuetto, M. F.; Thackeray, M. M.; Vissers, D. R.; Argriyou, D.; Loong, C. K.; Christensen, L. *J. Power Sources* **1997**, *68*, 570.
(6) Piffard, Y.; Leroux, F.; Guyomard, D.; Mansot, J. L.; Tournoux, M. *J. Power Sources* **1997**, *68*, 698.
(7) Chuang, P. Y.; Hu, Ch. *Mater. Chem. Phys.* **2005**, *92*, 138.
(8) Long, J. W.; Dunn, B.; Rolison, D. R.; White, H. S. *Chem. Rev.* **2004**, *104*, 4463.
(9) Wang, Y.; Takahashi, K.; Shang, H. M.; Lee, K. H.; Cao, G. Z. *J. Phys. Chem. B* **2005**, *109*, 3085.
(10) Wang, Y.; Cao, G. Z. *Chem. Mater.* **2006**, *18*, 2787.
(11) Sugantha, M.; Ramakrishnan, P. A.; Hermann, A. M.; Warmsingh, C. P.; Ginley, D. S. *Int. J. Hydrogen Energy* **2003**, *28*, 597.
(12) Xu, C. L.; Bao, S. J.; Kong, L. B.; Li, H.; Li, H. L. *J. Solid State Chem.* **2006**, *179*, 1351.
(13) Hill, L. L.; Verbaere, A.; Guyomard, D. *J. Electrochem. Soc.* **2003**, *150*, 135.
(14) Zhou, Y. K.; He, B. L.; Zhang, F. B.; Li, H. L. *J. Solid State Electrochem.* **2004**, *8*, 482.
(15) Chiu, K. F.; Lin, H. C.; Lin, K. M.; Chen, C. C. *J. Electrochem. Soc.* **2006**, *153*, A1992.

10.1021/cm702033z CCC: $40.75
Published on Web 01/10/2008

also demonstrated an initial capacity of 300 mAh/g;[16] however, the assembly of nanowires into electrodes was unwieldy. The present research demonstrates an uncomplicated and rapid approach to growing nanowall arrays of hydrous manganese dioxide by a template-free electrochemical deposition method. The morphology and structure of such nanowall arrays can be readily controlled by the externally applied electric voltage and the growth time. The resultant untreated nanowall arrays of hydrous manganese dioxide demonstrated an initial discharge capacity of 270 mAh/g and remained at 220 mAh/g at the 50th charge/discharge cycle in Li^+ ions intercalation measurements.

2. Experimental Section

The precursor solutions were made by dissolving manganese acetate, $Mn(CH_3COO)_2 \cdot 4H_2O$ (99+%, Alfa Aesar), and anhydrous sodium sulfate, Na_2SO_4 (99%, J.T. Baker), into DI water in a concentration of 0.1 M for both manganese acetate and sodium sulfate. The solution was stirred at room temperature for 1 h to ensure the complete dissolution of both solutes prior to electrodeposition experiment. Pt films sputter-coated on silicon substrates were used as both cathode for the growth of nanowall arrays of hydrous manganese oxide and anode as a counter electrode. The two electrodes were separated by a constant distance of 20 mm, and the deposition was carried out at a constant voltage ranging from −1.2 to −2.2 V for 15 min. A thin layer of golden-colored film was formed at the cathode, and gas bubbles were also generated at the cathode during the electrodeposition. The pH value of the electrolyte solutions was checked and found to remain unchanged at 6.5 before and after electrodeposition. This golden-colored film on the cathodic Pt substrate was air-dried in a fume hood with reduced pressure for 24 h and was not subjected to any further treatment, including annealing. The deposited films on the cathode Pt substrates were characterized by means of X-ray diffraction (XRD, Philips PW 1820), thermogravimetic analysis (TGA7, Perkin-Elmer), X-ray photoelectron spectroscopy (XPS, ESCA 210, VG Scientific Ltd.), and scanning electron microscopy (SEM, JSM 7000, Philips JEOL).

The electrochemical properties of the deposited films on the cathode Pt-coated substrates were conducted using a conventional three-electrode system. Platinum foil was used as the counter electrode with an Ag/AgCl electrode employed as the reference electrode and 1 M $LiClO_4$ in propylene carbonate as the electrolyte solution for Li^+ ions intercalation experiments. Chronopotentiometric measurements were carried out by using CHI 605B electrochemical station (CHI. Inc.) to determine the Li^+ ions intercalation capacity and charge/discharge cyclic behavior. The electric potential was controlled between 0.1 and −1.4 V versus the standard Ag/AgCl reference electrode, and the current was maintained at 0.1 mA/cm^2 for all the electrochemical measurements.

3. Results and Discussion

Figure 1a shows the typical XRD pattern of a manganese oxide film on a Pt-coated substrate, which indicates that the film possessed low crystallinity. Besides a broad peak around 19° from the glass used for XRD measurement and peaks at 40°, 47°, and 68° assigned to Pt, there are several peaks with very low intensity. A careful examination of all the manganese oxide XRD patterns enabled us to find out that the chemical compound was most likely ϵ-MnO_2 (Powder Diffraction File No. 12-141) which also had low crystallinity, and the peaks could not be indexed. Although the XRD pattern in Figure 1a was from a film deposited at −1.8 V, variation of deposition voltage, duration, and the electrolyte concentration did not result in a significant change of the XRD patterns.

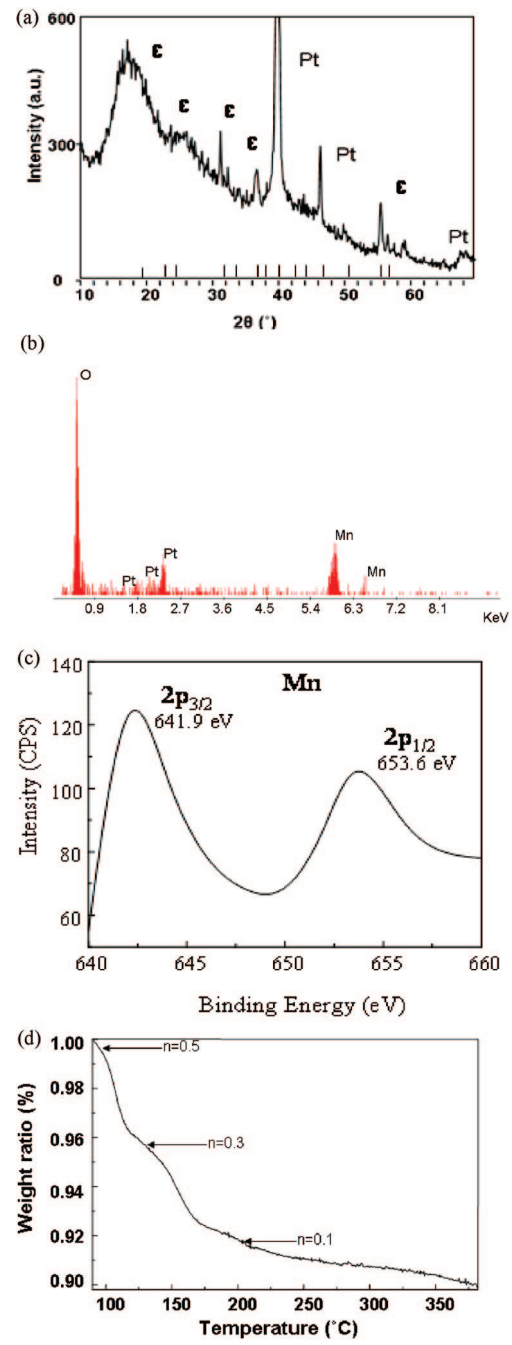

Figure 1. (a) X-ray diffraction pattern of hydrous manganese oxide grown at −1.8 V on platinum substrate for 15 min after ambient drying for 24 h without any heat treatment (standard peak positions of ϵ-MnO_2were marked at the bottom of XRD pattern). (b) Energy dispersive X-ray spectroscopy pattern of hydrous manganese oxide deposited at −1.8 V. (c) High-resolution XPS spectra of Mn $2p_{3/2,1/2}$ for −1.8 V nanowall arrays treated by air-drying. (d) Thermogravimetric curve of the −1.8 V nanowall arrays in air with a heating rate of 10 °C/min.

Energy dispersive X-ray spectroscopy (EDX) analyses (Figure 1b) revealed that the film consisted of manganese and oxygen, whereas no other chemical elements, including

(16) West, W. C.; Myung, N. V.; Whitacre, J. F.; Ratnakumar, B. V. *J. Power Sources* **2004**, *126*, 203.

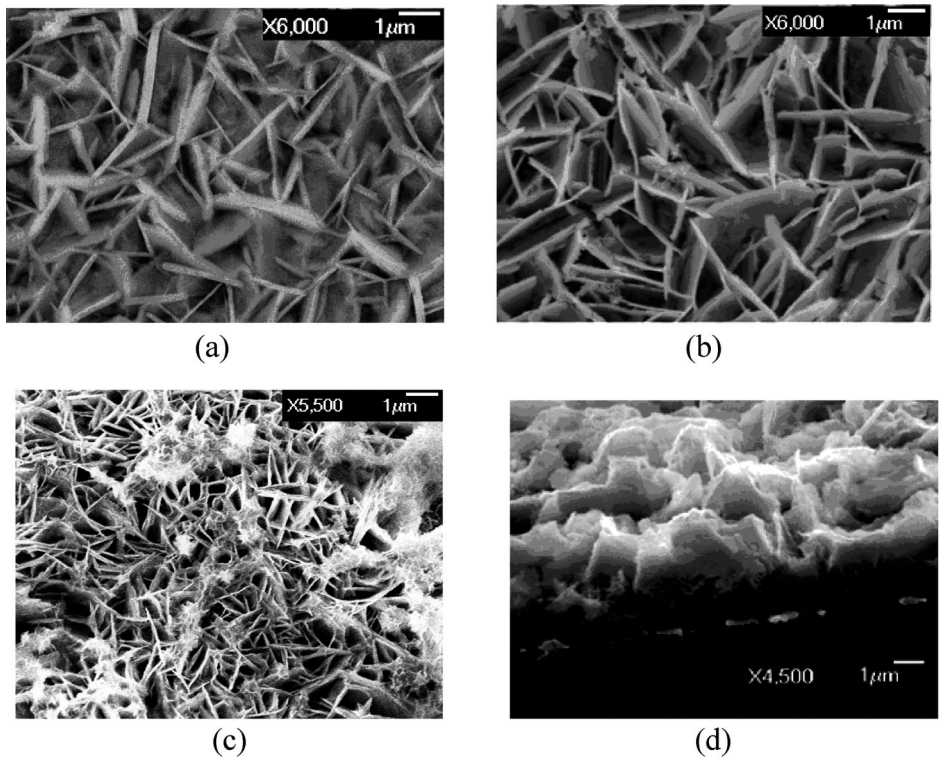

Figure 2. SEM images of nanowall arrays deposited at different voltages for 15 min: (a) top view of −1.2 V deposited nanowall arrays, (b) top view of −1.8 V nanowall arrays, (c) top view of −2.2 V nanowall arrays, and (d) side view of −1.8 V deposited nanowall arrays.

sodium or sulfur, were detectable. Further experiments with X-ray photoelectron spectroscopy (XPS) for high-resolution scan of Mn $2p_{3/2,1/2}$ found the binding energy peaks of $2p_{3/2}$ located at 641.9 eV and $2p_{1/2}$ located at 653.6 eV, as shown in Figure 1c; pure MnO_2 peak-pair ($2p_{3/2}$, 641.9 eV and $2p_{1/2}$, 653.5 eV) pattern could fit the spectra very well, revealing the energy state of only Mn^{4+}, existing in the form of MnO_2 bonded ions. So XRD, EDX, and XPS analyses collectively indicated that the deposited films consisted of manganese dioxide without appreciable impurity of other elements.

Figure 1d is the TGA curve of −1.8 V deposited sample which was degassed and dried at reduced pressure for 24 h, with powder peeled off the substrate for thermogravimetric measurement, showing ∼10% weight loss in the temperature ranging between 90 and 380 °C in air with a heating rate of 10 °C/min, which is attributed to the dehydration of the hydrous manganese dioxide, $MnO_2 \cdot nH_2O$. This result is very similar to the water content in hydrous manganese dioxide reported by Franger et al.[17] The deposited films were calculated to have a chemical composition of $MnO_2 \cdot nH_2O$ with $n = 0.53$ (≈ 0.5).

Figure 2 shows SEM images of $MnO_2 \cdot 0.5H_2O$ films deposited on Pt-coated substrates with an externally applied voltage varied between −1.2 and −2.2 V. The morphologies of nanowall arrays deposited at different voltages varied. Nanowall arrays deposited at both −1.2 V (Figure 2a) and −1.8 V (Figure 2b) showed homogeneous morphology, while the sample deposited at −2.2 V (Figure 2c) consisted of both nanowall arrays and some sporadically dispersed clusters of 1 μm in size. In the homogeneous nanowall arrays, the nanowall thickness varied from 50 to 100 nm. Similarly, the depth of the deposited nanowall structures changed appreciably when the applied voltage was varied from −1.2 to −1.8 V at identical deposition times of 15 min. The depth of the nanowall arrays deposited under −1.8 V was found to be ∼2.5 μm, while the −1.2 V deposited film only about 500 nm. When the growth time using −1.2 V increased to 2 h, the depth of nanowall arrays did not change significantly with a depth less than 1 μm. It was later found that −1.2 V nanowall arrays were not stable when subjected to Li^+ ions intercalation experiments as they dissolved into the electrolyte solution, while both samples grown under −1.8 and −2.2 V were stable during the electrochemical tests. Although it is not known at the moment what caused such a difference in electrochemical stability, the nanowalls deposited at −1.2 V may not be dense and thus were readily dissolved into the electrolyte solution. To solve this problem, different manganese salts will be tried in the precursor solution to modify the surface chemistry of the −1.2 V deposition. The cross-section SEM image shown in Figure 2d revealed that the nanowall structure was deposited with no continuous film at the interface between the Pt film and the $MnO_2 \cdot 0.5H_2O$ nanowall arrays. It should also be noted that this nanowall structure was more a pyramid structure with broader base than a "honeycomb" one with a uniform thickness from top to bottom.

The potentiostatic method deposition at cathode employed in this investigation, like the galvanostatic or potentiostatic three-electrode deposition at the anode,[18,19] can develop three-dimensional nanostructure; however, their growth

(17) Franger, S.; Bach, S.; Farcy, J.; Ramos, J. P.; Baffier, N. *J. Power Sources* **2002**, *109*, 262.

(18) Wu, M. S.; Chiang, P. C. *Electrochem. Commun.* **2006**, *8*, 383.

(19) Zhou, Y. K.; Toupin, M.; Be'langer, D.; Brousse, T.; Favier, F. *J. Phys. Chem. Solids* **2006**, *67*, 1351.

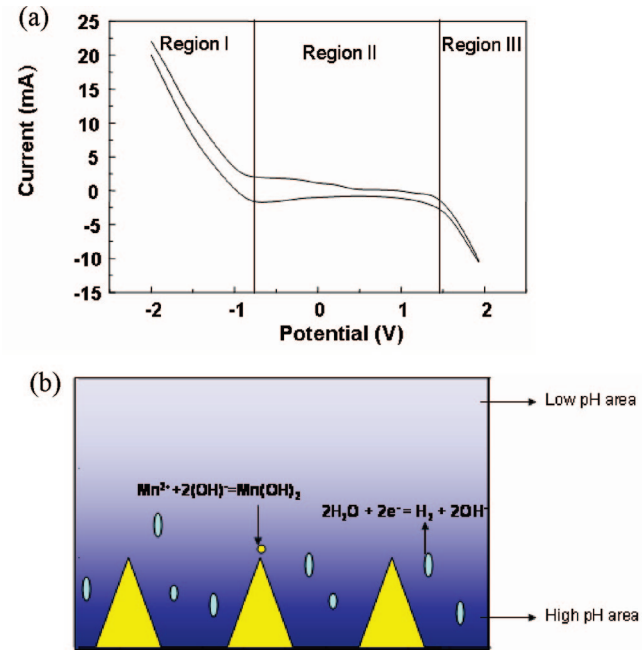

Figure 3. (a) Cyclic voltammetry curve of a 0.1 M sodium sulfate aqueous solution with a pH of 6.5, showing the reactions of water electrolysis. Region I: $2H_2O + 2e^- = H_2 + 2OH^-$; region II: no electrolysis of H_2O; region III: $2H_2O = O_2 + 4H^+ + 4e^-$. (b) Schematics showing the proposed growth mechanism of manganese hydroxide nanowall structure on cathodes due to the increased pH value resulting from water electrolysis.

mechanisms were quite different. For example, in anodic deposition, the formation of manganese dioxide came from the direct oxidation of Mn^{2+} to Mn^{4+} and thus was through a true electrochemical process at the interface between the anode and electrolyte solution. However, the cathodic deposition of hydrous manganese dioxide resulted from different chemical reactions. Instead of direct oxidation of Mn^{2+} to form oxide, the formation of hydrous manganese dioxide detailed herein was the result a sequential process that occurred at the surface or in the vicinity of the cathode, which included the electrolysis of water at the cathode surface, the increase of local pH at the vicinity of the cathode, reaction with OH^-, and then precipitation of manganese hydroxide on the cathode.[20,21] Manganese hydroxide further oxidized and decomposed to hydrous manganese dioxide when exposed to drying.

In order to understand the electrochemical reactions during the deposition process, cyclic voltammetry curve was measured with Pt-coated Si substrates as both cathode and anode, and platinum film was also used as the reference electrode. The electrolyte was 0.1 M sodium sulfate aqueous solution with a pH of 6.5. The voltage scan range was from −2 to 2 V versus platinum with a scan rate of 0.1 V/s. Figure 3a revealed that water electrolysis occurred when the cathodic potential was below −0.8 V versus platinum, resulting in the formation of both hydrogen gas and hydroxyl ions, as indicated as region I. Such a reaction resulted in an increase in pH in the vicinity of the cathode. Water electrolysis occurred at the anode as well when the electrode potential rose higher than ∼1.4 V versus platinum to form oxygen gas and protons as well as a reduction of pH value at the vicinity of anode. However, the overall pH of the electrolyte solution would remain unchanged. A duplicated CV test using the same cathode and anode but Ag/AgCl as reference electrode showed that the hydrogen gas formed around −0.6 V and the oxygen gas formed around 1.6 V, proving the cathodic property of the deposition.

Initially, the Mn^{2+} cations within the electrolyte solution were attracted to the negative polarity of the cathode surface, and then the local pH would change in the vicinity of cathode as a result of the electrolysis of water, which resulted in the precipitation of manganese hydroxide as schematically indicated in Figure 3b. As reported previously,[22] when the local pH reached 8 and above, the following reaction would happen.

$$Mn^{2+} + 2OH^- = Mn(OH)_2 \quad (1)$$

This deposition mechanism is similar to the growth of vanadium oxide nanorod arrays from VO_2^+ solution reported in the literature.[23,24] The combination of simultaneous release of hydrogen gas bubbles from the cathode surface and precipitation of $Mn(OH)_2$ in the vicinity prevented a compacted organization of the deposit on the cathode surface. Instead, nanostructured porous films or nanowall arrays of manganese hydroxide were formed. As to the initial deposition sites of the interface between the Pt film and $MnO_2 \cdot 0.5H_2O$ nanowall arrays, considering that the deposition was achieved through a precipitation induced by the change of local pH value as a result of water electrolysis on the surface of cathode, it was unlikely that a dense or continuous film would form at the bottom. A dense film would block the direct charge transfer between the cathode and water molecules. The release of H_2 gas bubbles as a byproduct of water electrolysis from the interface between the cathode and electrolyte would also hinder the formation of a continuous dense film at the bottom.

Manganese hydroxide is not a stable compound in the presence of oxygen; thus, $Mn(OH)_2$ is readily oxidized to a mixture of Mn_3O_4 and MnO_2, the ratio of which depends on the oxidation conditions such as different oxygen absorption levels and pH values according to the literature.[22] In our experiment, only MnO_2 was detected by the XPS data, indicating the oxidation to MnO_2 during deposition and subsequent drying processes through the following reaction:[22]

$$2Mn(OH)_2 + O_2 = 2MnO_2 + 2H_2O \quad (2)$$

No literature has so far been reported about the fabrication of manganese dioxide nanowall structure through this cathodic electrochemical route, and the method reported here is very promising for the fabrication of nanostructure electrodes considering its easy control of operation and chemical purity.

The resultant nanowall arrays of hydrous manganese dioxide deposited at −1.8 V were subjected to a systematic electrochemical analysis. The sample mass was estimated

(20) Nagarajan, N.; Humadi, H.; Zhitomirsky, I. *Electrochim. Acta* **2006**, *51*, 3039.
(21) Ho, W. H.; Yen, S. K. *J. Electrochem. Soc.* **2005**, *152*, 506.
(22) Nichols, A. R.; Walton, J. H. *J. Am. Chem. Soc.* **1942**, *64*, 1866.
(23) Cao, G. Z. *J. Phys. Chem. B* **2004**, *108*, 19921.
(24) Takahashi, K.; Limmer, S. J.; Wang, Y.; Cao, G. Z. *Jpn. J. Appl. Phys.* **2005**, *44*, 662.

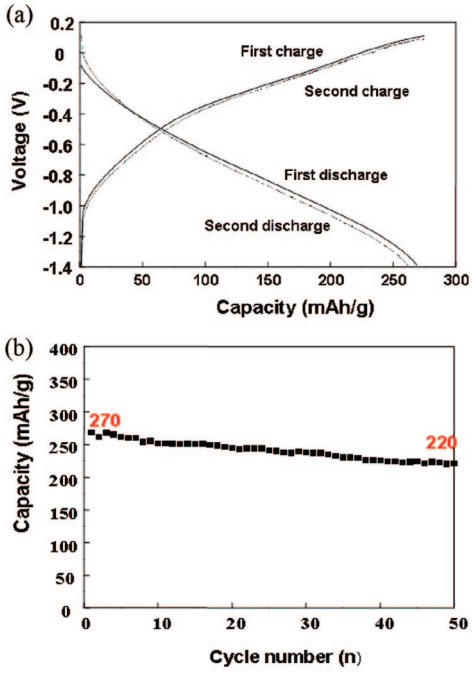

Figure 4. (a) Chronopotentiometric curves showing the Li^+ ions intercalation behaviors and capacities of hydrous manganese oxide nanowall arrays deposited at −1.8 V in the first and second charge/discharge cycles. (b) Li^+ ions discharge capacity as a function of charge/discharge cycles between the potential of 0.1 and −1.4 V vs Ag/AgCl at a specific current density of 0.1 mA/cm^2.

to be 0.45 mg by using an electronic microbalance to get the weight difference between pristine substrate and that with deposited sample after drying. Figure 4a displays and compares the first two discharge and charge curves of nanowall arrays. The nanowall electrode showed excellent discharge properties with a discharge capacity of 270 mAh/g in its first charge/discharge cycle at a rate of 0.1 mA/cm^2 (C/2, 76 mAh/g), i.e., corresponding to a lithium intercalation ratio of about 0.85 Li^+ per MnO_2, the same as reported sol–gel prepared manganese dioxide.[17] Additionally, the reversible capacity was also as high as 260 mAh/g in the second cycle, thus exhibiting good reversibility. The discharge capacity of the hydrous nanowall manganese dioxide was higher than other reported hydrous manganese dioxide measured at an even lower current density of 61.4 mAh/g.[25] Beyond the absolute value of the discharge capacities at various charge/discharge cycles, the high reversibility (nearly 100% Coulombic efficiency) of the nanowall arrays electrode also promised it a favorable battery cathode material.

Figure 4b summarizes the discharge capacities of the nanowall arrays of hydrous manganese dioxide deposited at −1.8 V over the first 50 cycles. Demonstrated is an initial discharge capacity of 270 mAh/g followed by a small gradual loss of capacity from the early cycles. However, even at the 50th cycle, the capacity was maintained at 220 mAh/g, displaying fine stability during cycling. The SEM image in Figure 5 of the nanowall arrays after 50 charge/discharge cycles revealed a likely explanation for the loss in capacity. It is likely that the exposed surface at the electrolyte−oxide interface may have gradually dissolved during cycling, in

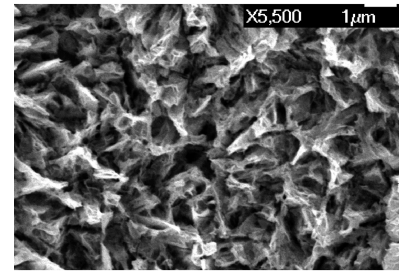

Figure 5. SEM image of the −1.8 V deposited nanowall arrays after 50 cycles of charge/discharge test.

the SEM image standing out as the disappearance of nanowall structure tips. This may result from erosion of the active manganese dioxide surface due to reactions with atmospheric water absorbed into the electrolyte.[26] Thus, available active manganese dioxide compound was getting less and less, creating the capacity degradation.

The enhanced discharge capacity in nanowall array electrodes is readily attributed to the increase in surface area for the faradaic reaction and short facile diffusion paths for Li^+ ions. Similar improvements in performance due to increase of surface area of active material were reported on nanostructured electrodes of vanadium oxides.[27] The roughly amorphous structure of hydrous manganese dioxide offers additional advantages. In well crystallized electrode materials, Li^+ ions intercalation is often accompanied with lattice structure distortion,[28] leading to significant capacity fading with successive charge/discharge cycles, whereas an approximately amorphous structure is less well packed and thus possesses greater ability for structural accommodation as well as more open free space during Li^+ ions intercalation and diffusion.

4. Conclusions

Nanowall arrays of $MnO_2 \cdot 0.5H_2O$ were readily grown by cathodic electrodeposition of manganese hydroxide as a result of water electrolysis-induced increase in local pH at the cathode surface. The morphological features of the 3-dimensional nanostructures were controlled by variation in the externally applied electric potential. The nanowall arrays, experimentally characterized as $MnO_2 \cdot 0.5H_2O$, demonstrated excellent Li^+ ions intercalation properties with a high capacity of 270 mAh/g due to its increased surface area, short facile diffusion paths, and generally amorphous composition.

Acknowledgment. This work has been supported in part by National Science Foundation (DMI-0455994) and Air Force Office of Scientific Research (AFOSR-MURI, FA9550-06-1-032). Dr. Ying Wang is acknowledged for her valuable advice on the electrochemical measurements. Prof. David Castner and staff in NESAC/BIO lab, University of Washington, are owed special thanks for their help in the XPS measurement and analyses.

CM702033Z

(25) Xu, J. J.; Jain, G.; Yang, J. *Electrochem. Solid-State Lett.* **2002**, *5*, 152.

(26) Pan, L. J.; Pu, L.; Shi, Y.; Song, S. Y.; Xu, Z.; Zhang, R.; Zheng, Y. D. *Adv. Mater.* **2007**, *19*, 461.

(27) Wang, Y.; Takahashi, K.; Lee, K. H.; Cao, G. Z. *Adv. Funct. Mater.* **2006**, *16*, 1133.

(28) Morales, J.; Sánchez, L.; Tirado, J. L. *J. Solid State Electrochem.* **1998**, *2*, 420.